



# Stability regions of fractional systems in the space of perturbed orders

Milan Rapać, Rachid Malti

## ► To cite this version:

Milan Rapać, Rachid Malti. Stability regions of fractional systems in the space of perturbed orders. IET Control Theory and Applications, 2019, 13 (16), pp.2610-2619. <10.1049/iet-cta.2018.6350>. <hal-02525798>

**HAL Id: hal-02525798**

**<https://hal.science/hal-02525798v1>**

Submitted on 16 Oct 2023

**HAL** is a multi-disciplinary open access archive for the deposit and dissemination of scientific research documents, whether they are published or not. The documents may come from teaching and research institutions in France or abroad, or from public or private research centers.

L'archive ouverte pluridisciplinaire **HAL**, est destinée au dépôt et à la diffusion de documents scientifiques de niveau recherche, publiés ou non, émanant des établissements d'enseignement et de recherche français ou étrangers, des laboratoires publics ou privés.



HAL Authorization

# On stability regions of fractional systems in the space of perturbed orders

 ISSN 1751-8644  
 doi: 0000000000  
 www.ietdl.org

 Milan R. RAPAĆ<sup>1</sup> Rachid MALTP<sup>2</sup>
<sup>1</sup> Computing and Control Department, Faculty of Technical Sciences, University of Novi Sad, Serbia.

<sup>2</sup> Univ. Bordeaux, IMS – UMR 5218 CNRS, France.

\* E-mail: {firstname.lastname}@ims-bordeaux.fr

**Abstract:** When dealing with fractional order systems, perturbations in differentiation orders arise frequently due to issues with floating point arithmetics, or due to imprecisions of various order estimation algorithms. This paper establishes new results regarding stability/instability of fractional systems with perturbed differentiation orders, knowing the related properties of their unperturbed counterparts. First of all, starting from a point in the space of differentiation orders, sufficient stability/instability conditions of all systems with differentiation orders varying along a line segment with a prescribed direction are established. Then, a continuation procedure is developed allowing computation of the maximum perturbation (along some given direction) which guaranties that the number of zeros in the closed right-half plane of the characteristic function remain unchanged. Finally, sufficient conditions are established guarantying stability/instability of all systems having differentiation orders within a domain. The established results allow concluding on the stability of incommensurate fractional transfer functions. They are illustrated by a number of examples, including an experimental one.

## 1 Introduction

Stability of fractional systems has been attracting a lot of interest during the last two decades in different fields of engineering and science. In [1, 2], fractional calculus was used for modeling general diffusive phenomena in semi-infinite planar, spherical, and cylindrical media. Moreover, in electrochemistry, it is proven that the diffusion of charges in acid batteries is governed by Randles models [3, 4] that involve a half order integrator. In semi-infinite thermal systems, it was shown in [5] that the exact solution of heat equation links thermal flux to a half order derivative of surface temperature on which the flux is applied. In rheology, stress in viscoelastic materials is proportional to a non integer derivative of deformation [6]. Foucault currents inside rotor bars in induction machines obey to diffusive phenomena modeled by fractional operators [7]. An advantage of continuous-time modeling is in straightforwardly estimating physical parameters even when the physics reveals systems governed by fractional differential equations. In this context and based on a fractional model, Gabano and Poinot [8] have successfully estimated thermal conductivity and diffusivity in a homogeneous medium.

It is well established that stability of linear time invariant fractional systems depends on the location of their poles in the complex plane which is a straightforward generalization of the rational case (conjectured by [9, 10, 11], proven in [12]). However, computing all the poles of a fractional system is not simple due to the plane cut and the limitation of arguments of the Laplace variable.

Powerful criteria have been proposed for testing stability of **fractional commensurate systems** since the seminal work by Matignon [11]. It allows concluding on the stability by locating system  $s^\nu$ -poles, where  $\nu$  is the commensurate order. Several other criteria resulting from Matignon's theorem have been established. For example, stability of fractional systems of the second kind may be deduced by checking the value of the pseudo-damping factor [13]. Stability analysis using Linear Matrix Inequalities (LMI) was established in [14, 15] as a direct extension of the second Lyapunov method. The LMI stability theorems can however be used only on commensurate fractional systems. An extension to large-scale fractional-order systems is proposed in [16]. A link with rational systems that possess the same stability properties is proposed in

[17, 18]. Extensions were also considered to fractional commensurate nonlinear systems in [19]. Multiple other references can be found in the survey paper [14].

Literature dedicated to the more general case of **incommensurate fractional systems** is not so mature. A numerical algorithm for stability testing based on Cauchy's principal theorem is proposed in [20]. The proposed algorithm is an improvement over the direct numerical application of Cauchy's argument principle but remains a sufficient stability condition. A method based on Nyquist theorem for testing stability of fractional systems is proposed in [21]. It is however limited to two differentiation orders in transfer function denominator. This result was extended to fractional systems with any number of differentiation orders in [22] by using nested closed-loops and addressing stability of the equivalent open-loop transfer functions. This method is based on a recursive closed-loop realization of the system and the application of Cauchy's argument principle on each loop of the realization. Computation of the number of poles in the right-half plane is done graphically on the images of Nyquist path. Although the authors propose a necessary and sufficient stability conditions, the proposed algorithm is quite difficult to implement numerically. In [23], the authors use a graphical method for determining stability region of incommensurate systems based on the analysis of stability boundary curves. The algorithm is quite difficult to implement numerically when multiple differentiation orders are involved. Lyapunov approach, based on continuous frequency representation [24, 25] may also be used for concluding on the stability of incommensurate fractional systems, though it is quite tedious.

Another way of tackling stability of fractional incommensurate systems is by considering **fractional uncertain systems** with uncertainties on the differentiation orders. However, many contributions [26, 27, 28, 29, 30, 31, 32, 33, 34, 35] consider uncertainties only on the coefficients and consider fixed differentiation orders. For example, in [35], the authors consider the problem of  $\mathcal{D}$ -stability of fractional interval systems by extending Kharitonov's theorem to fractional systems.

Tackling stability of fractional systems with perturbed differentiation orders is much more challenging, because such perturbations may change not only the commensurate order but also the commensurability condition. Stability test of fractional systems with uncertainties on differentiation orders was treated in the references [36, 37, 38, 39]. In [36] the authors showed the feasibility of their

method on a couple of examples using Kharitonov edge theorem with a small number of uncertainty intervals. They did not provide a rigorous proof for their result in the general case. In [37], edge polynomial sampling is used. Each uncertain parameter is sampled in its uncertainty interval and the sampling length of each parameter is a tuning parameter of the method. Then the root locus is checked in the stability region by mainly considering the roots of each sampled characteristic polynomial computed from sampled hypercubes. The smaller the sampling, the more precise the results, and the bigger the computational burden. This sampling dependent method provides only necessary stability conditions and its precision and computational complexity depend on the tuning parameters. In [38], it is shown that the Edge Theorem is not applicable for general interval fractional order systems. The authors show that the Edge Theorem can be applied when either the differentiation orders are fixed or the coefficients are fixed. Moreover, the authors use graphical methods to check the stability of interval fractional order systems with interval uncertainties in parameters and differentiation orders. The main difficulty of the method is to construct the boundary that depends on the uncertainty intervals in an efficient way. Inspired by all these methods, simpler criteria are established in [39] at the expense of some conservatism.

**Systems with perturbed differentiation orders** arise frequently in system identification using fractional models, especially when estimating differentiation orders [40, 41, 42]. Usually iterative algorithms are implemented such as gradient-based algorithms, because fractional models are nonlinear with respect to differentiation orders. In such algorithms, it is often necessary to check stability of intermediate models obtained at a given iteration. When differentiation orders are updated according to some value (corresponding to the step in the gradient algorithm), the system becomes frequently commensurate with a very low commensurate order close to the *machine epsilon*. In such conditions, it becomes impossible to check its stability using Matignon's theorem as illustrated in Section 2.

The problem of stability of fractional systems with perturbed differentiation orders, knowing stability/instability properties of their unperturbed counterparts is tackled here. As compared to the existing methods cited above [36, 37, 38, 39], this paper is based on the use Rouché's theorem from complex analysis and provides necessary conditions under which the characteristic functions of perturbed and unperturbed systems have the same number of zeros in the closed right-half complex plane. A continuation approach, along a line, allows obtaining necessary and sufficient stability conditions. The use of Hölder's inequality provides the hyperspace where stability is guaranteed. Moreover, the proposed approach allows a constructive investigation of boundaries of the stability/instability regions.

Preliminary results, corresponding to Theorem 3, were previously presented in [43] and [44]. More rigorous proofs and multiple extensions are provided in the present work.

First of all, stability conditions of systems with differentiation orders varying along a line segment in a prescribed direction are established in Section 3. As a first step, sufficient conditions are presented in the case when perturbations do not increase the highest differentiation order; then, an augmentation procedure is presented which enables utilization of the obtained result even in the case when the perturbation is not "highest-order-preserving". Section 3 is concluded with a continuation algorithm which allows computation of the maximum perturbation (along some given direction) guaranteeing that the number of zeros in the closed right-half plane of the characteristic equation will remain unchanged. In Section 4, sufficient conditions are established guaranteeing stability/instability of all systems having differentiation orders within a domain. Several numerical examples are used to illustrate the exposition. Finally, in Section 5 the proposed methodology is illustrated by investigating stability of an experimentally identified thermal plant. The paper finishes with a Conclusion.

## 1.1 Notation and Assumptions

$\mathbb{N}$ ,  $\mathbb{R}$  and  $\mathbb{C}$  are used to denote respectively the sets of natural, real and complex numbers, and  $\mathbb{R}_+ = \{x \in \mathbb{R} : x \geq 0\}$ . For an arbitrary vector  $\alpha$ , its  $i$ -th component is denoted as  $\alpha_i$ . Similarly, if  $\alpha_i$  is a component, then the entire vector will sometimes be denoted as  $(\alpha_i)_{i \in \{1..n\}}$ , where  $n$  is the number of components.

In several places, the well-know inequality is used

$$\left| \int_a^b m(t) dt \right| \leq \int_a^b |m(t)| dt \leq M(b-a), \quad (1)$$

where  $m$  is bounded integrable mapping,  $M = \max_{a \leq t \leq b} m(t)$ , and  $b > a \in \mathbb{R}$ . By the Integral Mean Value Theorem, if  $m$  is continuous on  $[a, b]$ , then there exists  $\tau \in (a, b)$  such that

$$\int_a^b m(t) dt = m(\tau)(b-a). \quad (2)$$

A symbolic representation of a dynamic system governed by a fractional differential equation is given in a **transfer function** form:

$$\frac{T(s, \beta)}{F(s, \alpha)} = \frac{\sum_{j=0}^k b_j s^{\beta_j}}{1 + \sum_{i=1}^n a_i s^{\alpha_i}}, \quad (3)$$

where  $\alpha = (\alpha_n, \alpha_{n-1}, \dots, \alpha_1)$  and  $\beta = (\beta_k, \beta_{k-1}, \dots, \beta_0)$  are vectors of differentiation orders. The denominator of (3),  $F(s, \alpha)$ , is referred to as the *characteristic function*. Some common assumptions are:

- A1. All differentiation orders are non-negative, so that  $\alpha \in \mathbb{R}_+^n$ ,  $\beta \in \mathbb{R}_+^{k+1}$ .
- A2. Transfer function (3) is strictly proper, i.e. high-frequency gain is zero, implying  $\max_j \beta_j < \max_i \alpha_i$ .
- A3. A branch cut line of the complex plane is chosen along the negative real axis including the branching point 0 and  $\infty$ , with arguments of  $s$  restrained to  $(-\pi, \pi]$ , for the function  $s \mapsto s^\nu$  to be analytic in the rest of the complex plane.

If numerator and denominator of  $\frac{T}{F}$  contain no common zeros, the stability is determined only by the location of the poles. It is therefore natural to formulate and solve the problem in terms of the characteristic function  $F$ . Note also that, if the transfer function (3) is commensurate of order  $\nu$ , then it can be rewritten as a ratio of two polynomials in  $s^\nu$

$$\frac{\tilde{T}(s^\nu)}{\tilde{F}(s^\nu)} = \frac{\sum_{j=0}^k b_j s^{j'\nu}}{1 + \sum_{i=1}^n a_i s^{i'\nu}}, \quad (4)$$

where  $j' = \frac{\beta_j}{\nu}$  and  $i' = \frac{\alpha_i}{\nu}$  are integers.

## 1.2 Stability

The stability addressed in this paper is the Bounded Input Bounded Output (BIBO). The system described by  $\frac{T}{F}$  in (3) is  $\mathcal{L}_p$ -stable,  $1 \leq p \leq \infty$ , if and only if

$$\sup_{u \in \mathcal{L}_p, u \neq 0} \frac{\|g \star u\|_p}{\|u\|_p} < \infty, \quad (5)$$

where  $\star$  stands for the convolution product,  $g$  the inverse Laplace transform (impulse response, or kernel) of  $\frac{T}{F}$  (or  $\frac{\tilde{T}}{\tilde{F}}$ ) and  $u(t)$  is the system input. The Bounded-Input-Bounded-Output (BIBO) stability

is defined as the  $\mathcal{L}_\infty$ -stability. In the case of fractional systems, Bonnet and Partington [12] extended the well-known result regarding stability of rational systems.

**Theorem 1** ([12]). *Let  $\frac{T}{F}$  be defined as in (3) with  $\alpha_n \geq \beta_k$ . Then  $\frac{T}{F}$  is BIBO stable if and only if  $\frac{T}{F}$  has no pole in the closed right-half plane  $\{s : \Re(s) \geq 0\}$  (in particular no pole of fractional order at  $s = 0$ ).*

This theorem, conjectured by [9, 10, 11], will be used later in this paper. Further, Matignon [11] established a very useful result regarding stability of commensurate fractional systems.

**Theorem 2** ([11] extended). *A commensurate transfer function  $\frac{\tilde{T}}{\tilde{F}}$  with a commensurate order  $\nu$ , as in (4), with  $\tilde{T}$  and  $\tilde{F}$  two coprime polynomials, is stable if and only if  $0 < \nu < 2$  and*

$$(\forall s \in \mathbb{C}) \quad \tilde{F}(s) = 0 \Rightarrow s \in \Sigma_{\nu \frac{\pi}{2}}, \quad (6)$$

where for all  $\phi \in [0, \pi]$

$$\Sigma_\phi = \{s \in \mathbb{C} : |\arg(s)| > \phi\}. \quad (7)$$

Matignon initially proved this theorem for  $0 < \nu < 1$ . The proof is extended in multiple references to the interval  $(1, 2)$ , see e.g. [13]. This theorem is extended further in [45] to delayed fractional systems of retarded and neutral type. Some further results on the stability of fractional systems with time delays can be found in [46, 47, 48, 49, 50].

Additionally, it is shown in [51] that a fractional system might be stable and yet have an infinite  $\mathcal{L}_2$ -norm impulse response (infinite energy). This result is extended to  $\mathcal{L}_p$ -norms,  $1 \leq p \leq \infty$ , in [52].

## 2 Problem formulation

First, start by formulating the problem on the characteristic function:

$$F(s, \alpha) = s^{\alpha_2} + 2s^{\alpha_1} + 1. \quad (8)$$

where  $\alpha = (\alpha_2, \alpha_1)$ . Theorem 2 is very useful for testing stability of fractional systems numerically. However, it does not apply to the incommensurate system  $F^{-1}(s, \alpha^1)$  with  $\alpha^1 = (\pi, \sqrt{2})$ .

Numerical representation of the real numbers gathered in  $\alpha^1$  using floating point arithmetics is however impossible. Only approximations of  $\alpha^1$ , such as  $\alpha^{1*} = (\pi^*, \sqrt{2}^*)$ , can be coded numerically. Hence,  $F^{-1}(s, \alpha^{1*})$  is commensurate with a commensurate order close to the *machine epsilon*, which is the maximum round-off error between a real number and its representation. When using double precision arithmetics, defined by the IEEE 754 standard, the *machine epsilon* is  $\epsilon = 2.22 \times 10^{-16}$ . Although testing stability of  $F^{-1}(s, \alpha^{1*})$  using Matignon's theorem is theoretically possible, it is infeasible in practice, because it would have required checking that all the roots of the polynomial:

$$\begin{aligned} F(s^{\frac{1}{\epsilon}}, \alpha^{1*}) &= s^{\frac{\pi^*}{\epsilon}} + 2s^{\frac{\sqrt{2}^*}{\epsilon}} + 1 \\ &= s^{1.41 \times 10^{16}} + 2s^{0.64 \times 10^{15}} + 1 \end{aligned} \quad (9)$$

belong to the sector  $\Sigma_{\epsilon \frac{\pi}{2}}$ .

Assume now that the differentiation orders are coded with three digit precision. The characteristic function  $F(s, \alpha^2)$  with  $\alpha^2 = (3.141, 1.414)$  is now commensurate of order 0.001. Testing its

stability requires computing all the roots of the polynomial

$$F(s^{10^{-3}}, \alpha^2) = s^{3141} + 2s^{1414} + 1 \quad (10)$$

and checking that they all belong to the sector  $\Sigma_{0.001 \frac{\pi}{2}}$ . This operation is numerically feasible, although time-consuming\* and the results should be considered with great caution because significant numerical errors may occur. Finally, assume that the differentiation orders are coded with one digit precision. Stability testing of the characteristic function  $F(s, \alpha^3)$ , with  $\alpha^3 = (3.2, 1.4)$ , requires computing all the roots of<sup>†</sup>:

$$F(s^{\frac{1}{0.2}}, \alpha^3) = s^{16} + 2s^7 + 1 \quad (11)$$

and checking that they all belong to the sector  $\Sigma_{0.2 \frac{\pi}{2}}$ . Computing numerically all the roots of the 16<sup>th</sup> degree polynomial (11) is much simpler, faster\*, and more reliable.

In this particular case, the question is whether it is possible to conclude on stability (resp. instability) of  $F^{-1}(s, \alpha^2)$ ,  $F^{-1}(s, \alpha^{1*})$ , and  $F^{-1}(s, \alpha^1)$  by testing the stability of  $F^{-1}(s, \alpha^3)$ . How far the orders of  $F^{-1}(s, \alpha^3)$  can be perturbed and yet guarantee the stability (resp. instability) of  $F^{-1}$ .

More generally, the addressed problem is the following: for given  $\alpha^A \in \mathbb{R}_+^n$ ,  $\alpha^B \in \mathbb{R}_+^n$ , and a given characteristic function  $F$  of (3) establish

- (i) a line (along the direction  $(\alpha^B - \alpha^A)$ ):  $\alpha(t) = \alpha^A + (\alpha^B - \alpha^A)t$  such that for all  $t < t_c$ ,  $F(s, \alpha^A)$  and  $F(s, \alpha(t))$  have the same number of zeros in the closed right-half plane,
- (ii) a region  $\Omega \subset \mathbb{R}_+^n$  centered at  $\alpha^A$  such that for all  $\alpha \in \Omega$ , the characteristic functions  $F(s, \alpha^A)$  and  $F(s, \alpha)$  have the same number of zeros.

The former problem is treated in Section 3 and the latter in Section 4.

## 3 Stability on a Line

Let  $\alpha^A, \alpha^B \in \mathbb{R}_+^n$  and let

$$\alpha(t) = \alpha^A + (\alpha^B - \alpha^A)t, \quad (12)$$

so that for an arbitrary  $t \in (0, 1)$ ,  $\alpha(t)$  is a point on the line segment connecting  $\alpha^A = \alpha(0)$  and  $\alpha^B = \alpha(1)$ . The question addressed in the present section is: *What is the biggest value of  $t$  so that  $F(s, \alpha^A)$  and  $F(s, \alpha(t))$  have the same number of zeros in the closed right-half plane?* Firstly, in Subsection 3.1, we consider sufficient conditions when the highest order in  $\alpha^B$  is smaller or equal to the highest order in  $\alpha^A$ . This constraint is alleviated later in Subsection 3.2. Finally, necessary and sufficient conditions are considered in Subsection 3.3.

\*Computing all the roots of a polynomial in MATLAB involves computing the eigenvalues of a Companion Matrix, which dimension equals polynomial's degree, via an iterative algorithm. Its complexity depends on the number of iterations. It takes around 50s on author's laptop to compute all the roots of (36) as compared to  $\approx 0.5ms$  to compute all the roots of (11). It is about  $10^5$  slower in the former case as compared to the latter.

<sup>†</sup> $\pi$  is approximated by 3.2 and  $\sqrt{2}$  by 1.4.

<sup>‡</sup>The commensurate order equals 0.2.

### 3.1 Perturbations not increasing the degree of $F$

**Definition 1.** For a given vector of differentiation orders  $\alpha \in \mathbb{R}_+^n$ , the set of all highest-order-preserving vectors is

$$\mathcal{S}_{hop}(\alpha) = \{\alpha' \in \mathbb{R}_+^n : \max_i \alpha_i \geq \max_i \alpha'_i\}.$$

**Theorem 3.** Let  $\alpha^A \in \mathbb{R}_+^n$ ,  $\alpha^B \in \mathcal{S}_{hop}(\alpha^A)$ , and  $F(s, \alpha)$  as in (3). Consider  $\alpha(t) \in \mathbb{R}_+^n$  given by (12), and let

$$S_F(j\omega, t) = \left( \int_0^t a_i(j\omega)^{\alpha_i(\tau)} \text{Ln}(j\omega) d\tau \right)_{i \in \{1, \dots, n\}}, \quad (13)$$

where  $\text{Ln}(s)$  is the principal value of the complex logarithm. A sufficient condition for  $F(s, \alpha^A)$  and  $F(s, \alpha(t))$  to have the same number of zeros in the closed right-half plane is that for all  $\omega > 0$

$$|F(j\omega, \alpha^A)| > \left| \int_0^t \frac{\partial F(j\omega, \alpha(\tau))}{\partial \tau} d\tau \right|, \quad (14)$$

or, equivalently,

$$|F(j\omega, \alpha^A)| > \left| \langle S(j\omega, t), \alpha^B - \alpha^A \rangle \right|, \quad (15)$$

where  $\langle \cdot, \cdot \rangle$  denotes the scalar product.

*Proof:* By applying the Fundamental Theorem of Calculus to  $F(s, \alpha(t))$  \* we find that for any given  $s \in \mathbb{C}$

$$F(s, \alpha(t)) = F(s, \alpha^A) + \int_0^t \frac{\partial F(s, \alpha(\tau))}{\partial \tau} d\tau, \quad (16)$$

where

$$\frac{\partial F(s, \alpha(\tau))}{\partial \tau} = \sum_{i=1}^n a_i s^{\alpha_i(\tau)} (\alpha_i^B - \alpha_i^A) \text{Ln}(s). \quad (17)$$

By applying Rouché's theorem [53], see the appendix,  $F(s, \alpha^A)$  and  $F(s, \alpha(t))$  have the same number of zeros within the closed right-half plane if

$$|F(s, \alpha^A)| > \left| \int_0^t \frac{\partial F(s, \alpha(\tau))}{\partial \tau} d\tau \right| \quad (18)$$

on the contour  $\mathcal{C}$  depicted in Fig. 1 with  $\varepsilon \rightarrow 0$  and  $R \rightarrow \infty$ . After inserting (17) into (18), and interchanging the order of integration and summation, the condition reads

$$|F(s, \alpha^A)| > \left| \sum_{i=1}^n \int_0^t a_i s^{\alpha_i(\tau)} \text{Ln}(s) d\tau (\alpha_i^B - \alpha_i^A) \right|, \quad (19)$$

or equivalently,

$$|F(s, \alpha^A)| > \left| \langle S_F(s, t), \alpha^B - \alpha^A \rangle \right|. \quad (20)$$

Consider separately three sub-contours: (i) the imaginary axis (without the origin), (ii) the “small” quarter-circle of radius  $\varepsilon$ , and (iii) the “big” quarter-circle of radius  $R$ . Notice that, due to symmetry of

(20), only the “upper” quadrant (with positive imaginary part of  $s$ ) needs to be considered.

i) On the upper part of the imaginary axis,  $s = j\omega$  with  $\omega > 0$ . In this case, (18) and (20) reduce to condition (14) (or equivalently (15)), stated in the Theorem.

ii) On the upper part of the “small” quarter-circle, the Laplace variable is substituted by  $s = \varepsilon e^{j\varphi}$ , with  $\varphi \in [0, \pi/2]$  and  $\varepsilon \rightarrow 0$ . Since  $\alpha(t) \in \mathbb{R}_+^n$ , the left-hand side of (20) approaches 1, while the right-hand side vanishes. To see this, note that (1) implies

$$\left| \int_0^t (\varepsilon e^{j\varphi})^{\alpha_i(\tau)} \text{Ln}(\varepsilon e^{j\varphi}) d\tau \right| \leq \left( \max_{0 < \tau < t} \varepsilon^{\alpha_i(\tau)} \left| \text{Ln}(\varepsilon) + j\frac{\pi}{2} \right| \right) t \quad \forall i \in \{1, \dots, n\}.$$

The obtained upper limit vanishes with  $\varepsilon$ , and so does the right-hand side of (14) and (15).

iii) On the upper part of the “big” quarter-circle, the Laplace variable is substituted with  $s = R e^{j\varphi}$ , with  $\varphi \in [0, \pi/2]$  and  $R \rightarrow \infty$ . For large values of  $R$ , the left-hand side of (19) grows with  $R^{\alpha_{\max}}$ , where  $\alpha_{\max} = \max_i \alpha_i^A$ . Note that by assumption  $\alpha(t) \in \mathcal{S}_{hop}$ , so that  $\alpha_{\max} \geq \max_i \alpha_i(t)$  for all  $t$ . To evaluate the asymptotic behavior of the right-hand side of (19), notice first that for any  $i \in \{1, \dots, n\}$

$$\left| \int_0^t (R e^{j\varphi})^{\alpha_i(\tau)} \text{Ln}(R e^{j\varphi}) d\tau \right| \leq \left( \int_0^t R^{\alpha_i(\tau)} d\tau \right) \left| \text{Ln}(R) + j\frac{\pi}{2} \right|.$$

By means of (2), the last inequality reads

$$\left| \int_0^t (R e^{j\varphi})^{\alpha_i(\tau)} \text{Ln}(R e^{j\varphi}) d\tau \right| \leq \left( R^{\alpha_i(\tau_i)} t \right) \left| \text{Ln}(R) + j\frac{\pi}{2} \right|,$$

for some  $\tau_i \in (0, t)$ . So that the right-hand side of (19) is upper bounded by

$$\sum_{i=1}^n a_i R^{\alpha_i(\tau_i)} (\alpha_i^B - \alpha_i^A) \left| \text{Ln}(R) + j\frac{\pi}{2} \right|. \quad (21)$$

Two separate cases must be considered: either (i)  $\alpha(t)$  decreases the highest order of  $\alpha$ , or (ii) it keeps the highest order constant. In the first case, all  $\alpha_i(\tau_i)$  are strictly smaller than  $\alpha_{\max}$ . In the second case, for some  $i$ ,  $\alpha_i(\tau_i)$  is constant and equals to  $\alpha_{\max}$ , but for that  $i$ ,  $\alpha_i^B - \alpha_i^A = 0$ , and the corresponding term does not contribute to the upper bound (21) or the right-hand side of (19). Either way, the upper bound (21) asymptotically grows as  $R^{\alpha'} \text{Ln}(R)$  for some  $\alpha' < \alpha_{\max}$ . Consequently, (19) is satisfied for sufficiently large  $R$ .  $\square$

**Theorem 4.** Under assumptions of Theorem 3, a sufficient condition for the characteristic functions  $F(s, \alpha^A)$  and  $F(s, \alpha(\tau))$  to have the same number of zeros in the closed right-half plane for all  $\tau \in [0, t]$  is

$$B(t) > t, \quad (22)$$

where

$$B(t) = \min_{\omega > 0} \frac{|F(j\omega, \alpha^A)|}{M(\omega, t)}, \quad (23)$$

$$M(\omega, t) = \max_{0 \leq \tau \leq t} \left| \frac{\partial F(j\omega, \alpha(\tau))}{\partial \tau} \right|. \quad (24)$$

\*Actually, the Fundamental Theorem of Calculus (FTC) is usually stated for real-valued functions. However, equation (16) is obtained by applying FTC separately to real and imaginary parts of  $F$ , and then combining the resulting real-valued expressions into a single complex-valued one.

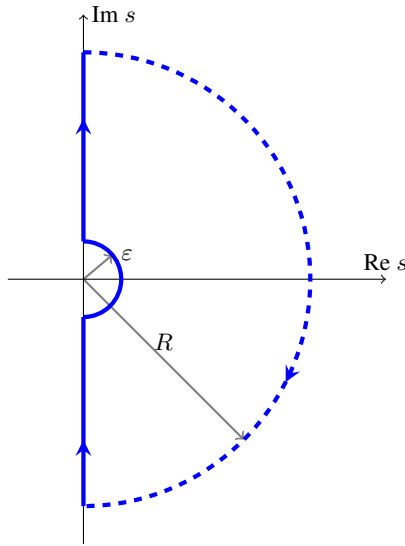


**Fig. 1:** Contour  $C$  used when applying the Rouché Theorem in the proof of Theorem 3.

*Proof:* Let us prove that (22) implies (15), so that the claim follows by application of Theorem 3. The following inequalities hold

$$\begin{aligned} t &< B(t) && \text{due to (22)} \\ &\leq \frac{|F(j\omega, \alpha^A)|}{M(\omega, t)} \quad (\forall \omega > 0) && \text{due to (23)} \\ &\leq \frac{|F(j\omega, \alpha^A)|}{\left| \frac{\partial F(j\omega, \alpha(\tau))}{\partial \tau} \right|} \quad (\forall \omega > 0, 0 \leq \tau \leq t) && \text{due to (24)} \end{aligned}$$

Therefore, (22) implies that

$$\begin{aligned} |F(j\omega, \alpha^A)| &> \left( \max_{0 \leq \tau \leq t} \left| \frac{\partial F(j\omega, \alpha(\tau))}{\partial \tau} \right| \right) t \quad (\forall \omega > 0) \\ &\geq \int_0^t \left| \frac{\partial F(j\omega, \alpha(\tau))}{\partial \tau} \right| d\tau \\ &\geq \left| \int_0^t \frac{\partial F(j\omega, \alpha(\tau))}{\partial \tau} d\tau \right|, \end{aligned}$$

and so, by Theorem 3,  $F(s, \alpha^A)$  and  $F(s, \alpha(t))$  have the same number of zeros in the closed right-half plane. Furthermore, since  $M(\omega, t)$  does not decrease with  $t$  (for any fixed  $\omega$ ),  $B(t)$  is a non-increasing function of  $t$ . Therefore, if  $B(t) > t$ , then  $B(\tau) > \tau$  for all  $0 \leq \tau \leq t$ .  $\square$

**Corollary 5.** Under assumptions of Theorem 4, let  $t_c$  be the smallest solution of

$$B(t_c) = t_c \quad (25)$$

then, for all  $0 \leq t < t_c$ ,  $F(s, \alpha^A)$  and  $F(s, \alpha(t))$  have the same number of zeros in the closed right-half plane.

**Example 1.** Consider  $F$  as in (8),  $\alpha^A = (3.2, 1.4)$ , and  $\alpha^B = (\pi, \sqrt{2})$ . By the application of Matignon's theorem,  $F(s, \alpha^A)$  is unstable. Is it possible to conclude on the instability of  $F(s, \alpha^B)$ ? Graphical evaluation of condition (25) is shown in Fig. 2. It leads to  $t_c \approx 0.067$ , which means that the critical value of the order vector is

$$\alpha_c = \alpha(t_c) \approx [3.1961, 1.4010].$$

The total step size in the space of differentiation order is  $t_c \|\alpha^B - \alpha^A\| \approx 0.0286$ . The system is guaranteed to be unstable for all  $\alpha(t)$  with  $0 \leq t < 0.067$ . Since  $t_c < 1$ , stability of  $\alpha^B$  remains inconclusive.

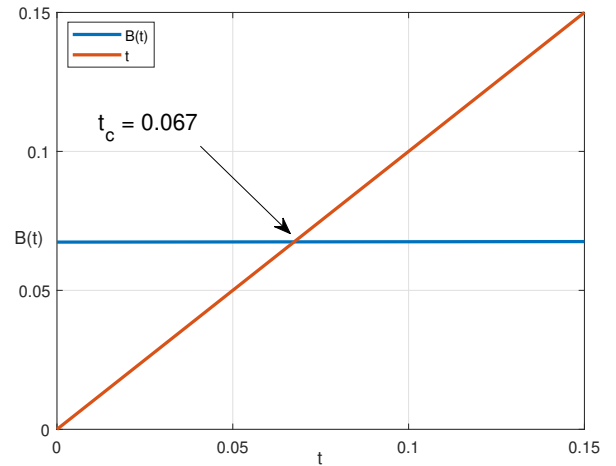


**Fig. 2:** Graphical evaluation of condition (25) in Example 1. The critical value  $t_c$  is obtained in the intersection of the two curves.

### 3.2 Perturbations increasing the degree of $F$

The principal difficulty with perturbations increasing the highest differentiation order is that (20) no longer holds for “large” values of  $s$ . More precisely, left-hand side of (19) is of a smaller order of magnitude than the right-hand side on the “big” semicircle. To circumvent this problem, the characteristic equation can be augmented with a “stable” multiplicative factor such that the highest differentiation order in the product is fixed.

**Theorem 6.** Consider  $\alpha^A, \alpha^B \in \mathbb{R}_+^n$ , together with  $F(s, \alpha)$  as in (3), and  $\alpha(t) \in \mathbb{R}_+^n$  given by (12). Let  $\Delta\alpha = \alpha^B - \alpha^A$ , and  $i^* = \operatorname{argmax}_i \alpha_i^A$ . Introduce

$$H_L(s, t) = (s^{1-t \frac{\Delta\alpha_{i^*}}{L}} + 1)^L, \quad (26)$$

$$F_L^*(s, \bar{\alpha}(t)) = F(s, \alpha(t)) H_L(s, t), \quad (27)$$

where  $L \in \mathbb{N}$ ,  $L \geq |\Delta\alpha_{i^*}|$ , and  $\bar{\alpha}$  is the transformed vector of differentiation orders, obtained by explicitly multiplying the two factors of (27). Let

$$t' = \sup\{t > 0 : i^* = \operatorname{argmax}_i \alpha_i(t)\},$$

and  $t'' = \min\{1, t'\}$ , then for all  $t \in (0, t'')$ :

- i)  $F_L^*(s, \bar{\alpha}(t))$  contains only positive powers of  $s$  which are all affine functions of  $t$
- ii) the highest power of  $s$  in  $F_L^*(s, \bar{\alpha}(t))$  is independent of  $t$ , and
- iii)  $F(s, \alpha(t))$  and  $F_L^*(s, \bar{\alpha}(t))$  have the same number of zeros in the closed right-half plane.

*Proof:* i) Since  $L > |\Delta\alpha_{i^*}|$  and  $|t| < 1$ ,  $H_L(s, t)$  contains only positive powers of  $s$ , so the same must be true for  $F_L^*$  as well. All powers of  $s$  appearing in  $F_L^*$  are sums of different powers of  $s$  appearing in  $H_L$  and  $F$ , both of which are affine functions of  $t$ .

ii) Since  $t < t'$ , the highest power of  $s$  in  $H_L$  is  $L - t\Delta\alpha_{i^*}$ , while the highest power in  $F$  is  $\alpha_{i^*}^A + t\Delta\alpha_{i^*}$ . Term with the highest power in the product  $F_L^*$  is therefore  $L + \alpha_{i^*}^A$ , which is independent of  $t$ .

iii) Due to Matignon's Theorem,  $H_L$  contains only zeros in the open left-hand side of the complex plane for all  $|t| < 1$ , so that the number of zeros in  $F$  and  $F_L^*$  which lie in the closed right-half plane is the same.  $\square$

**Remark 1.** Theorem 6 allows to interpret  $F_L^*(s, \bar{\alpha}(t))$  as a characteristic function, of the same form as the one appearing in (3), only

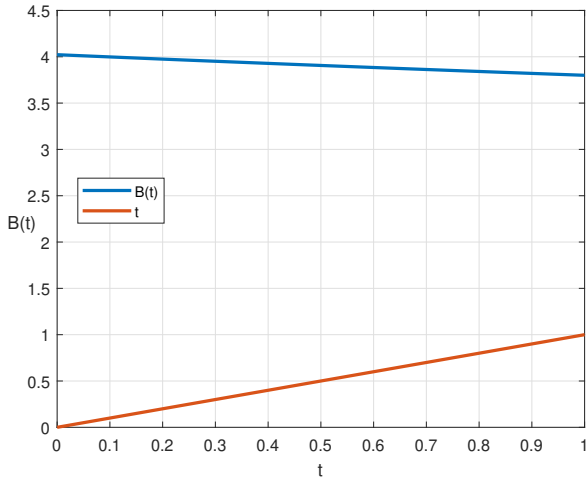


**Fig. 3:** Graphical evaluation of condition (25) in Example 2.

with  $\alpha$  replaced by  $\bar{\alpha}$ . Mapping  $\alpha \mapsto \bar{\alpha}$  is affine and the number of zeros in the closed right-half plane of  $F$  and  $F_L^*$  is the same; however, the highest power of  $s$  in  $F_L^*$  is fixed, so that stability of  $F$  can be investigated by applying Theorems 3 and 4 to  $F_L^*$ .

**Example 2.** Consider Example 1, but with a slightly modified initial point  $\alpha^A = (3.1, 1.4)$ . By the application of Matignon's theorem,  $F(s, \alpha^A)$  is stable. Is it possible to conclude on the stability of  $F(s, \alpha^B)$ ? Since  $\alpha_1^B > \alpha_1^A$ , it is impossible to directly apply Theorems 3 or 4. By choosing  $L = 1$ , the augmented characteristic polynomial of Theorem 6 becomes

$$F_1^*(s, \bar{\alpha}(t)) = s^{1+\alpha_2^A} + 2s^{1+\alpha_1^A+t(\Delta\alpha_1-\Delta\alpha_2)} + s^{1-t\Delta\alpha_2} + s^{\alpha_2^A+t\Delta\alpha_2} + 2s^{\alpha_1^A+t\Delta\alpha_1} + 1, \quad (28)$$

with

$$\bar{\alpha}(t) = (1 + \alpha_2^A, 1 + \alpha_1^A + t(\Delta\alpha_1 - \Delta\alpha_2), 1 - t\Delta\alpha_2, \alpha_2^A + t\Delta\alpha_2, \alpha_1^A + t\Delta\alpha_1).$$

The upper allowable parameter value  $t''$  of Theorem 6 is obtained from

$$\alpha_2^A + t\Delta\alpha_2 > \alpha_1^A + t\Delta\alpha_1,$$

which is fulfilled for all positive values of  $t$ . Therefore,  $t' = +\infty$  and  $t'' = 1$ . Applying Theorem 4 to  $F_L^*$ , allows concluding that  $F_L^*(s, \bar{\alpha}(t))$  and  $F_L^*(s, \bar{\alpha}(0))$  have the same number of zeros in the closed right-half plane. Illustration is given in Fig 3. In conclusion, since  $F^{-1}(s, \alpha^A)$  is stable, so is  $F^{-1}(s, \alpha^B)$ , and so is  $F^{-1}(s, \alpha(t))$  for all  $t \in [0, 1]$ .

### 3.3 Continuation : Necessary and Sufficient Conditions

When applying Corollary 5, it is possible to claim that  $F(s, \alpha^A)$  and  $F(s, \alpha^B)$  have the same number of zeros in the closed right-half plane only if  $t_c > 1$ . However,  $t_c \leq 1$  does not imply that the number of closed right half-plane zeros is different. In fact, it is possible to choose some  $t^1 < t_c$  and reapply Corollary 5 starting from  $\alpha(t^1)$  by proceeding in the same direction. If necessary, the procedure can be repeated multiple times, as described in Algorithm 1.

**Theorem 7.** Consider the sequence  $\{t^i\}$  generated by Algorithm 1 with  $\varepsilon = 0$ . If the sequence is finite, we assume that it has been extended by repeating the last element ad infinitum.

### Algorithm 1 The continuation algorithm.

---

**Require:**  $\alpha^0 \in \mathbb{R}_+^n$   
**Require:**  $\Delta\alpha \in \mathbb{R}^n$   
**Require:**  $0 < \rho < 1$   
**Require:**  $\varepsilon \geq 0$

```

 $t^0 \leftarrow 0$ 
 $i \leftarrow 0$ 
loop
  Set  $\alpha^A = \alpha^i, \alpha^B = \alpha^i + \Delta\alpha$ 
  Apply Corollary 5 to obtain  $t_c$ .
  if  $t_c < \varepsilon$  then
    return
  end if
   $t^{i+1} \leftarrow t^i + \rho t_c$ 
   $i \leftarrow i + 1$ 
   $\alpha^{i+1} \leftarrow \alpha^i + \rho t_c \Delta\alpha$ 
  if  $\alpha^{i+1} \neq \max\{\alpha^{i+1}, 0\}$  then
     $\alpha^{i+1} \leftarrow \max\{\alpha^{i+1}, 0\}$ 
  end if
end loop

```

---

\*In the listing above, max is used as a component-wise operation.

- i) If  $\{t^i\}$  converges to some  $t^*$ , then  $F(s, \alpha^0)$  and  $F(s, \alpha(t))$  have the same number of zeros in the closed right-half plane for all  $t < t^*$ .
- ii) If  $\{t^i\}$  converges to some  $t^*$  such that  $\alpha(t^*) > 0$ , then  $F(s, \alpha(t^*))$  has at least one zero on the imaginary axis.
- iii) If  $\{t^i\}$  diverges to  $+\infty$ , then for all  $t > 0$ ,  $F(s, \alpha^0)$  and  $F(s, \alpha(t))$  have the same number of zeros in the closed right-half plane.

*Proof:* Note first that the sequence  $\{t^i\}$  is non-negative, non-decreasing; it can therefore either converge to some non-negative  $t^*$ , or diverge to  $+\infty$ .

Parts i) and iii) follow immediately by construction:  $F(s, \alpha(t))$  has an unchanging number of zeros in the closed right-half plane for all  $t \in [0, t^i]$  and any  $i \in \mathbb{N} \setminus \{0\}$ .

Assume now that  $t^*$  is the limit, and that  $\alpha(t^*) > 0$ . The only reason for the algorithm not to continue beyond  $t^*$  is the  $t_c$  computed by Corollary 5 with  $\alpha^A = \alpha(t^*)$  would happen to be zero, i.e. if  $B(0) = 0$ . This could happen either if  $M(\omega, 0)$  is infinite for some  $\omega$ , or if  $|F(j\omega, \alpha(t^*))|$  is zero for some  $\omega$ . Since  $M$  is bounded,  $F(s, \alpha(t^*))$  must attain zero at least at one point on the imaginary axis.  $\square$

**Corollary 8.** Under assumptions of Theorem 4, necessary and sufficient condition for  $F(s, \alpha^0)$  and  $F(s, \alpha(t))$  to have the same number of zeros in the closed right-half plane, for all  $t \in [0, 1]$  (i.e. on the entire line-segment connecting  $\alpha^A$  to  $\alpha^B$ ) is that the sequence  $\{t^i\}$  generated by Algorithm 1 either converges to  $t^* > 1$  or diverges.

**Remark 2.** Conditions stated in Theorem 3 are only sufficient, due to the fact that the proof is based on the Rouché's Theorem. An additional layer of conservatism is introduced in Theorem 4 (and also in Theorem 6), due to upper-bounding of an appropriate integral. However, by repeated application of those claims the conservatism issue is removed, and Algorithm 1 gives both sufficient and necessary conditions under which the number of zeros in the closed right-hand side is preserved (Theorem 7).

**Remark 3.** Algorithm 1 should be applied with care. The procedure itself does not pose any self-regulatory mechanism that would allow it to recover from an accidental jump over the ideal limit  $t^*$ , which might be caused by roundoff errors, or other numerical problems. In particular, if  $t^i$  accidentally becomes larger than  $t^*$  then there is no mechanism to stop it growing further away. This may lead to false conclusions, since for  $t > t^*$ , the number of zeros in the closed



**Table 1** Output sequence of Algorithm 1 in Example 3 with an instable initial point  $\alpha^A$

$i$	$t^i$	$\alpha^i$
0	0	(3.2000, 1.4000)
1	0.0636	(3.1963, 1.4009)
2	0.0855	(3.1950, 1.4012)

**Table 2** Output sequence of Algorithm 1 in Example 3 with a stable initial point  $\alpha^{A_2}$

$i$	$t^i$	$\alpha^i$
0	0	(3.1000, 1.4000)
1	3.2272	(3.2342, 1.4459)
2	3.6300	(3.2510, 1.4516)
3	3.6927	(3.2536, 1.4525)

right-half plane of  $F(s, \alpha(t))$  and  $F(s, \alpha(0))$  is probably different. Parameter  $\rho$  is introduced for this very reason; it reduces the step size and forces the following step to start from a numerically more favorable position. Parameter  $\varepsilon$  forces the algorithm to stop once it becomes sufficiently close to the stability boundary.

**Example 3.** Let's apply the continuation approach to  $F(s, \alpha)$  in (8) by choosing the target point  $\alpha^B = (\pi, \sqrt{2})$  and three different initial points  $\alpha^{A_1}, \alpha^{A_2}, \alpha^{A_3}$ . For each initial point, Algorithm 1 is applied with  $\alpha^0 = \alpha^{A_i}$ ,  $\Delta\alpha = \alpha^B - \alpha^{A_i}$ , and  $\rho = 0.95$ .

First, consider the unstable initial point  $\alpha^{A_1} = (3.2, 1.4)$  of Example 1. Applying Algorithm 1 with a precision of  $\varepsilon = 0.005^*$  one obtains the sequence reported in Table 1. This sequence converges to  $\alpha^2 = (3.1950, 1.4012)$  without reaching the target point. Applying ii) of Theorem 7 allows to conclude that  $F(s, \alpha^2)$  has at least one zero on the imaginary axis. Theorem 7 does not allow to state whether beyond  $\alpha^2$ , on the line joining  $\alpha^{A_1}$  to  $\alpha^B$ , the number of zeros is bigger or smaller. Henceforth, the stability of  $F(s, \alpha^B)$  remains inconclusive.

Consider now the stable initial point  $\alpha^{A_2} = (3.1, 1.4)$  of Example 2. The sequence obtained by applying Algorithm 1 with a precision of  $\varepsilon = 0.1^\dagger$  is reported in Table 2. The limit point  $\alpha^3 = (3.2536, 1.4525)$  is well beyond the target point  $\alpha^B$  (on the given line). This confirms that  $F(s, \alpha^B)$  and  $F(s, \alpha^{A_2})$  have the same number of closed right half-plane zeros. Henceforth,  $F^{-1}(s, \alpha^B)$  is stable.

Next, for illustration purposes, consider the initial point  $\alpha^{A_3} = (1, 1)$ . The obtained sequence of  $\{\alpha^i\}$  is reported graphically in Fig. 4, along the dashed line.

Finally, instead of considering a single direction from  $\alpha^{A_3} = (1, 1)$  to  $\alpha^B$ , consider multiple directions to identify the stability boundary in the  $(\alpha_2, \alpha_1)$ -plane. Apply the continuation approach, from the initial point  $\alpha^{A_3}$ , and consider  $N$  radially equidistant directions,

$$\alpha^{B,\ell} = \alpha^{A_3} + (\cos(\varphi_\ell), \sin(\varphi_\ell)),$$

where  $\varphi_\ell = -\frac{\pi}{4} + \frac{\ell}{N}\pi$ ,  $0 \leq \ell \leq N$ , and  $N = 60$ . The results are shown in Fig. 4, where the limit point of each continuation process is indicated by a black dot. The obtained results are verified by repeated application of Matignon's Theorem to commensurate points  $(i\nu, j\nu)$  inside and outside the stability boundary plotted in Fig. 4 (where  $\nu = 0.2$  is used).

It is not possible to prove formally that all points in the interior of the "stability margin" of Fig.4 preserve stability. Although a dense

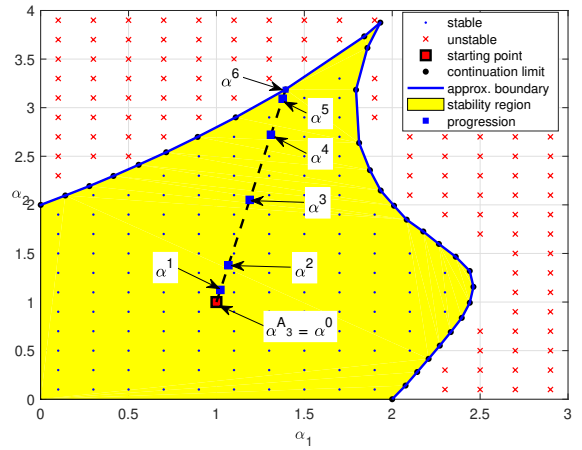


**Fig. 4:** Stability margin obtained by the continuation approach. Continuous line denotes the stability boundary obtained numerically in the  $(\alpha_2, \alpha_1)$  plane.

set of directions starting from  $\alpha^{A_3}$  can be chosen, this set cannot be infinitesimal. This is why results regarding stability/instability within a domain are required.

#### 4 Stability within a domain

Previous results have all been used to establish line segments in the parameter space in which the number of zeros in the closed right half-plane is unchanged. In many cases, however, it is more convenient to have a region of guaranteed stability/instability around a given point. In a slightly more general formulation, we assume that the differentiation order vector is an *affine* function of a perturbation vector  $\epsilon \in \mathbb{R}^r$ , with  $r \leq n$ , i.e. that there exists a matrix  $P \in \mathbb{R}^{n,r}$  such that

$$\alpha(\epsilon) = \alpha^A + P\epsilon. \quad (29)$$

The problem is to determine a region  $\Omega \subset \mathbb{R}^r$  such that for all  $\epsilon \in \Omega$  the number of zeros in the closed right half-plane of  $F(s, \alpha^A)$  and  $F(s, \alpha(\epsilon))$  is the same. Often, the perturbations act directly on the differentiation orders, so that  $r = n$ ,  $P$  is the identity matrix, and  $\alpha(\epsilon) = \alpha^A + \epsilon$ . In other cases, for example if one applies augmentation as in Theorem 6, the dependence of  $\alpha$  on  $\epsilon$  is not trivial.

**Theorem 9.** Let  $\alpha^A \in \mathbb{R}_+^n$ ,  $F(s, \alpha)$  as in (3) and

$$G_F(j\omega, \epsilon) = \left( \frac{\partial F(j\omega, \alpha(\epsilon))}{\partial \epsilon_i} \right)_{i \in \{1, \dots, r\}}. \quad (30)$$

Let  $\alpha(\epsilon)$  be defined as in (29). Choose any  $p, q \geq 1$  such that  $1/p + 1/q = 1$ , and any  $\varepsilon_q > 0$ . A sufficient condition for the characteristic functions  $F(s, \alpha^A)$  and  $F(s, \alpha(\epsilon))$  to have the same number of zeros in the closed right-half plane for all  $\alpha(\epsilon) \in \mathcal{S}_{hop}(\alpha^A)$  such that  $\|\epsilon\|_q \leq \varepsilon_q$  is

$$B_q(\|\epsilon\|_q) > \varepsilon_q, \quad (31)$$

where

$$B_q(\varepsilon) = \min_{\omega > 0} \frac{|F(j\omega, \alpha^A)|}{M_q(\omega, \varepsilon)}, \quad (32)$$

$$M_q(\omega, \varepsilon) = \max_{\|\epsilon\|_q \leq \varepsilon} \|G_F(j\omega, \epsilon)\|_p. \quad (33)$$

\*A small  $\varepsilon$  is chosen in Algorithm 1 because  $\alpha^A$  is very close to the stability limit.

†A bigger  $\varepsilon$  is chosen here, because  $\alpha^{A_2}$  is now further from the stability limit.



*Proof:* Due to (31) and (32), for any  $\epsilon$  such that  $\|\epsilon\|_q \leq \varepsilon_q$

$$\min_{\omega>0} \frac{|F(j\omega, \alpha^A)|}{M_q(\omega, \|\epsilon\|_q)} > \varepsilon_q \geq \|\epsilon\|_q ,$$

implying that for all  $\omega > 0$ ,

$$|F(j\omega, \alpha^A)| > M_q(\omega, \|\epsilon\|_q) \|\epsilon\|_q .$$

Taking into account (33), for all  $\omega > 0$  and any  $\|\epsilon\|_q \leq \varepsilon_q$

$$|F(j\omega, \alpha^A)| > \|G_F(j\omega, \epsilon)\|_p \|\epsilon\|_q .$$

Using Hölder inequality [54], product of the norms on the right-hand side can be lower-bounded by the absolute value of the inner product, so that for all  $\omega > 0$  and all  $\epsilon$  such that  $\|\epsilon\|_q \leq \varepsilon_q$

$$\|G_F(j\omega, \epsilon)\|_p \|\epsilon\|_q \geq |\langle G_F(j\omega, \epsilon), \epsilon \rangle| .$$

Thus, by direct application of the basic properties of integrals

$$\|G_F(j\omega, \epsilon)\|_p \|\epsilon\|_q \geq \left| \int_0^1 \langle G_F(j\omega, \epsilon(t)), \epsilon(t) \rangle dt \right| ,$$

and therefore

$$|F(j\omega, \alpha^A)| > \left| \int_0^1 \langle G_F(j\omega, \epsilon(t)), \epsilon(t) \rangle dt \right| .$$

Finally, the last expression can equivalently be rewritten as

$$|F(j\omega, \alpha^A)| > \left| \int_0^1 \frac{\partial F(j\omega, \alpha(\epsilon(t)))}{\partial t} dt \right| .$$

Thus, by starting from the conditions of the present claim, we arrive at the condition (14), which concludes the proof.  $\square$

**Remark 4.** Theorem 9 can be interpreted as a procedure in which one considers the most conservative bound, looking at all possible directions from  $\alpha_A$ .

**Corollary 10.** Under assumptions of Theorem 9, let  $\varepsilon$  be the smallest solution of

$$B_q(\varepsilon) = \varepsilon \quad (34)$$

then  $F(s, \alpha^A)$  and  $F(s, \alpha^A + P\epsilon)$  have the same number of zeros in the closed right-half plane for all  $\epsilon$  such that  $\|\epsilon\|_q < \varepsilon$ .

**Remark 5.** Theorem 9 is somewhat conservative: it is based on two inequalities (Rouché's and Hölder's), none of which is tight. It is however possible to apply a form of continuation, in this case as well, simply by re-applying Theorem 9 or Corollary 10 to edge points of the previously computed stability regions. Unfortunately, the procedure would lead to domains of irregular shapes, and efficient manipulations of those is beyond the scope of the present paper.

**Example 4.** Let us revisit Example 1 by determining a guaranteed stability/instability domain around two different initial points. Introduce perturbations directly into the vector of differentiation orders, so that  $\alpha = \alpha^A + \epsilon$  (i.e.  $P$  is the identity matrix).

By choosing  $\alpha^{A1} = (3.2, 1.4)$ . Areas of guaranteed instability obtained for different values of  $q$  are shown in Figure 5. Because the augmentation is not used in this Example, only differentiation orders  $\alpha$  such that  $\alpha_2 < \alpha_2^{A1}$  are considered.

The widest area, delimited by thick blue line, is obtained by application of Theorem 4 sequentially, along a number of arrays starting from  $\alpha^{A1}$  (in the same manner used to obtain stability "region" in

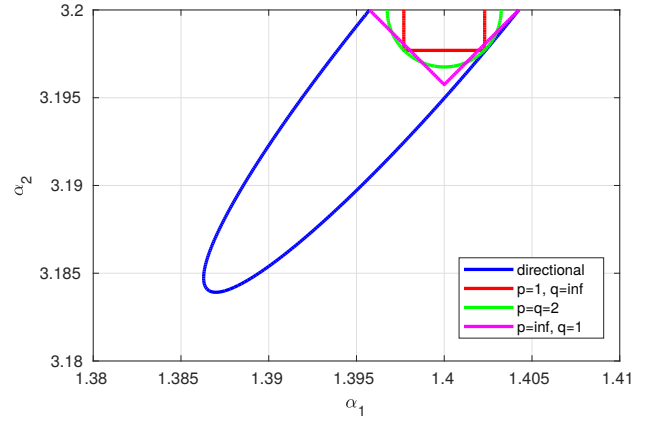


**Fig. 5:** Areas of guaranteed instability surrounding point  $\alpha^A = (3.2, 1.4)$  computed in Example 4. The “directional” contour is obtained by application of Theorem 4 (without continuation).

the last part of Example 3). Continuation is *not* used. The figure illustrates results obtained by *one-step* application of Theorem 4. For this reason, the obtained instability contour is denoted as “directional”.

The remaining three contours are obtained by application of Theorem 9 (more precisely Corollary 10). The two rectangular areas are obtained with  $q = 1$  and  $q = \infty$ , respectively, while the circular area corresponds to  $q = 2$ .

This example clearly illustrates the fact that Theorem 9 can be obtained from Theorem 4, by considering each array in the parameter space. Once stability/instability bounds are found along each direction, the one having the smallest  $q$ -norm is chosen. Thus, for any  $q$ , the region obtained by Theorem 9 is a subset of the region obtained by sequential application of Theorem 4, with the bounds touching each other in at least one point. This point is, in fact, minimal with respect to  $q$ -norm on the “directional” contour.

Theorem 9 remains true if  $F(s, \alpha)$  is formally replaced by  $F^*(s, \bar{\alpha})$ . Therefore, it remains valid when applied to the extended form of the characteristic equation (27). In this way, it is possible to obtain areas of guaranteed stability/instability in which the highest differentiation order is allowed to increase as well. Figure 6 shows area of guaranteed stability surrounding point  $\alpha^A = (3.1, 1.4)$  for different values of  $q$  obtained in this way. In particular, Theorem 9 is applied to the augmented characteristic polynomial (28) in which  $t\Delta\alpha_1 \equiv \epsilon_1$  and  $t\Delta\alpha_2 \equiv \epsilon_2$ . Shaded area in the same figure is the instability “area” previously depicted in Figure 5. Clearly, the stability region obtained around point  $(3.1, 1.4)$  and instability area surrounding point  $(3.2, 1.4)$  do not overlap, as expected. Moreover, the point  $(\pi, \sqrt{2})$  clearly falls into the stability area.

## 5 Application to stability verification of an identified model of a thermal plant [41]

Consider a long aluminium rod shown in Fig. 7. The input signal is a thermal flux generated by a resistor glued at one end and the output signal is the temperature of the rod measured at a distance  $x = 0.5\text{cm}$  from the heated end using a platinum probe. To ensure a unidirectional heat transfer, the entire surface of the rod is insulated.

The system is driven to a steady-state temperature by injecting a constant flux density of  $\phi = 5\text{kWm}^{-2}$  for a sufficiently long period. Then a pseudo-random-binary-signal is applied with a flux variation of  $\pm 5\text{kWm}^{-2}$  around the constant flux of  $5\text{kWm}^{-2}$ . A delay of 4 samples (2s) is observed between the output and the input.

In [55], a theoretical model of the aluminum rod, obtained by solving heat equation under some simplifying assumptions, was compared to experimental data. Among the simplifying assumptions, the rod was assumed to be perfectly isolated. The theoretical model was found to be commensurate of order 0.5. It was also shown that fractional models are more compact than rational models: higher

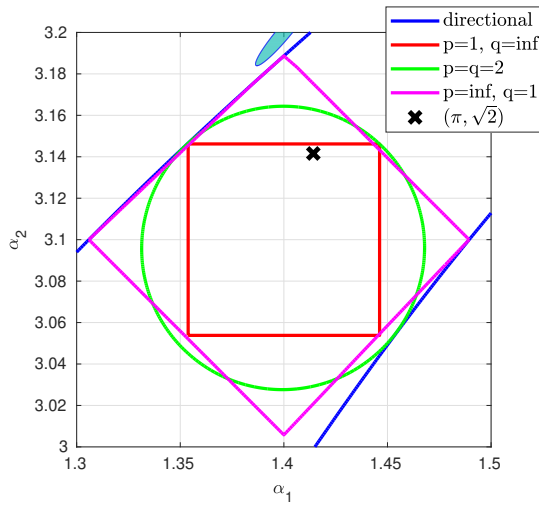


**Fig. 6:** Areas of guaranteed stability surrounding point  $\alpha^A = (3.1, 1.4)$  obtained in Example 4. The “directional” contour is obtained by application of Theorem 4 (without continuation). The small shaded area is the instability “region” surrounding point  $(3.2, 1.4)$ .

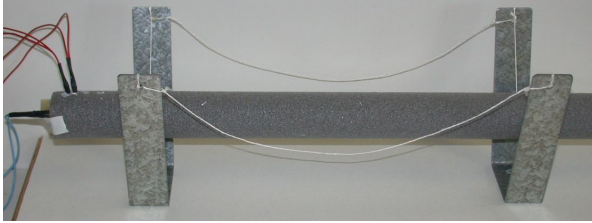


**Fig. 7:** Insulated long aluminium rod heated by a resistor

order rational models are required to get comparable results to fractional models. However, since the aluminum rod reaches a steady state temperature, it is not perfectly insulated. Consequently, there is no reason to have a commensurate order of 0.5 nor to have an integrator as in the physical model [55].

In [41], a black box model was identified by minimizing the  $\ell_2$ -norm of the output error. First of all, a commensurate differentiation order was optimized and the optimal order was found to be around 0.6. Then the commensurability condition was released and the differentiation orders were further adjusted. Output of the obtained model

$$G(s, \alpha) = \frac{3.09 \times 10^{-3}}{263.4s^{\alpha_2} + 88.78s^{\alpha_1} + 1} e^{-2s}, \quad (35)$$

with  $\alpha = (\alpha_2, \alpha_1)$ ,  $\alpha_1 = \alpha_1^{\text{opt}} = 0.593$  and  $\alpha_2 = \alpha_2^{\text{opt}} = 1.186$ , is compared to experimental measurements on Fig. 8.

The objective of this example is to examine the stability of the obtained model (35). Brut force application of Matignon’s theorem would require checking that all roots of the characteristic function of  $G(s^{0.001})$ ,

$$F_G(s^{0.001}, \alpha) = 263.4s^{1186} + 88.78s^{593} + 1, \quad (36)$$

belong to the sector  $\Sigma_{10^{-3}\pi}^{\frac{\pi}{2}}$ . As indicated in Section 2, this operation is numerically feasible, although time-consuming and the results should be considered with great caution because significant numerical errors may occur.

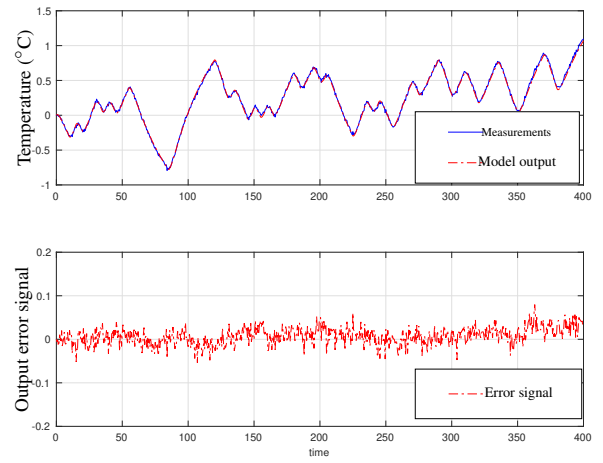


**Fig. 8:** Time-domain responses plotted on validation data ( $y_1$  stands for the commensurate model output (35) and  $y_2$  for the non commensurate model output of Table 4)

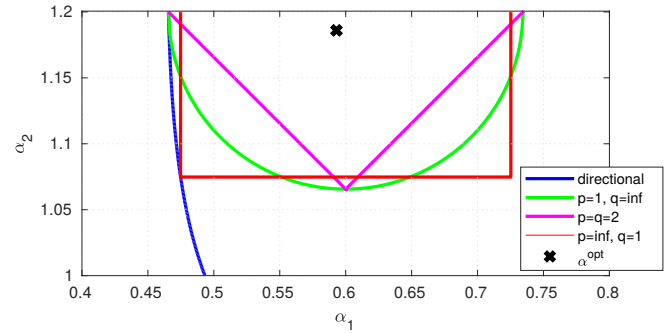


**Fig. 9:** Regions of guaranteed stability surrounding point  $(\alpha_1, \alpha_2) = (1.2, 0.6)$  obtained using different combinations of norms.

Instead, stability is first determined for  $(\alpha_2, \alpha_1) = (1.2, 0.6)$ , which is performed by investigating the characteristic function,

$$F_G(s^{0.1}, (1.2, 0.6)) = 263.4s^{12} + 88.78s^6 + 1. \quad (37)$$

Starting from this initial stable point, the surrounding stability region is obtained by means of the procedure derived in Section 4, and illustrated in Fig. 9. Since the desired perturbations do not increase the overall degree of the characteristic equation in this case, augmentation is not necessary, but the computed stability region contains  $\alpha_2 \leq \alpha_2^{\text{opt}}$  only.

Alternatively, one can start from a stable point  $(\alpha_1, \alpha_2) = (1.1, 0.6)$ , apply augmentation in the same manner as in Example 2, and then proceed as in Section 4 in order to obtain stability region. The result is plotted in Fig 10. In either case, the point  $\alpha^{\text{opt}} = (1.186, 0.593)$  is clearly inside the stability region.

## 6 Conclusions

Important results are established in this paper allowing to conclude on the stability/instability of fractional transfer functions having perturbed differentiation orders, knowing the stability/instability of the unperturbed ones. Stability of incommensurate transfer functions can be deduced from the established results. For that purpose, (i) a necessary and sufficient stability/instability conditions are established along a line segment on a prescribed direction, (ii) sufficient stability/instability conditions are established within a domain.

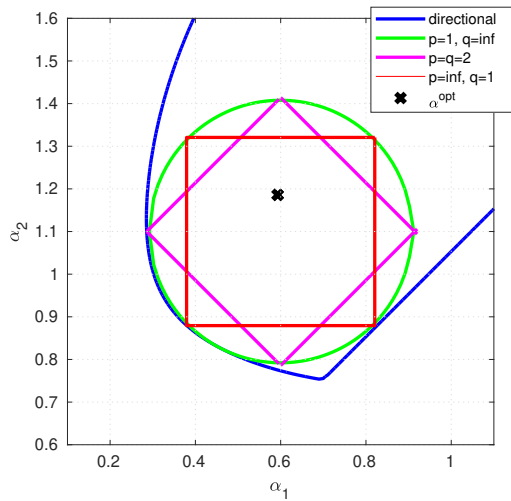


**Fig. 10:** Regions of guaranteed stability surrounding point  $(\alpha_1, \alpha_2) = (1.1, 0.6)$  obtained using different combinations of norms.

## 7 References

- 1 K. Oldham and J. Spanier, "The replacement of Fick's laws by a formulation involving semi-differentiation," *Electro-anal. Chem. Interfacial Electrochem*, vol. 26, pp. 331–341, 1970.
- 2 —, *The fractional calculus - Theory and Applications of Differentiation and Integration to Arbitrary Order*. Academic Press, New-York and London, 1974.
- 3 S. Rodrigues, N. Munichandraiah, and A.-K. Shukla, "A review of state of charge indication of batteries by means of A.C. impedance measurements," *Journal of Power Sources*, vol. 87, pp. 12–20, 2000.
- 4 J. Sabatier, M. Aoun, A. Oustaloup, G. Grégoire, F. Ragot, and P. Roy, "Fractional system identification for lead acid battery state charge estimation," *Signal Processing*, vol. 86, no. 10, pp. 2645–2657, 2006.
- 5 J.-L. Battaglia, O. Cois, L. Puigsegur, and A. Oustaloup, "Solving an inverse heat conduction problem using a non-integer identified model," *Int. J. of Heat and Mass Transfer*, vol. 44, no. 14, pp. 2671–2680, 2001.
- 6 N. Heymans and J. Bauwens, "Fractal rheological models and fractional differential equations for viscoelastic behavior," *Rheologica Acta*, vol. 33, p. 219, 1994.
- 7 A. Benchellal, S. Bachir, T. Poinot, and J.-C. Trigeassou, "Identification of a non-integer model of induction machines," in *1st IFAC Workshop on Fractional Differentiation and its Applications (FDA)*, Bordeaux, France, 2004.
- 8 J.-D. Gabano, T. Poinot, and H. Kanoun, "Identification of a thermal system using continuous linear parameter-varying fractional modelling," *IET Control Theory & Applications*, vol. 5, no. 7, pp. 889–899, May 2011.
- 9 S. Skaar, A. Michel, and R. Miller, "Stability of viscoelastic control systems," *Automatic Control, IEEE Transactions on*, vol. 33, no. 4, pp. 348–357, Apr 1988.
- 10 A. Oustaloup, *La dérivation non-entière: théorie, synthèse et applications*. Hermès - Paris, 1995.
- 11 D. Matignon, "Stability properties for generalized fractional differential systems," *ESAIM proceedings - Systèmes Différentiels Fractionnaires - Modèles, Méthodes et Applications*, vol. 5, 1998.
- 12 C. Bonnet and J. Partington, "Coprim factorizations and stability of fractional differential systems," *Systems & Control Letters*, vol. 41, no. 3, pp. 167 – 174, 2000.
- 13 R. Malti, X. Moreau, F. Khemane, and A. Oustaloup, "Stability and resonance conditions of elementary fractional transfer functions," *Automatica*, vol. 47, no. 11, pp. 2462–2467, 2011.
- 14 J. Sabatier, M. Moze, and C. Farges, "LMI stability conditions for fractional order systems," *Computers & Mathematics with Applications*, vol. 59, no. 5, pp. 1594 – 1609, 2010.
- 15 C. Farges, M. Moze, and J. Sabatier, "Pseudo-state feedback stabilization of commensurate fractional order systems," *Automatica*, vol. 46, no. 10, pp. 1730 – 1734, 2010.
- 16 Y. Boukal, M. Darouach, M. Zasadzinski, and N. Radhy, "Large-scale fractional-order systems: stability analysis and their decentralised functional observers design," *IET Control Theory Applications*, vol. 12, no. 3, pp. 359–367, 2018.
- 17 M. Tavazoei and M. Haeri, "A note on the stability of fractional order systems," *Mathematics and Computers in Simulation*, vol. 79, no. 5, pp. 1566 – 1576, 2009. [Online]. Available: <http://www.sciencedirect.com/science/article/pii/S0378475408002437>
- 18 H. Nasiri and M. Haeri, "How bibo stability of Iti fractional-order time delayed systems relates to their approximated integer-order counterparts," *Control Theory Applications, IET*, vol. 8, no. 8, pp. 598–605, May 2014.
- 19 R. Zhang, G. Tian, S. Yang, and H. Cao, "Stability analysis of a class of fractional order nonlinear systems with order lying in  $(0, 2)$ ," *ISA Transactions*, vol. 56, pp. 102 – 110, 2015. [Online]. Available: <http://www.sciencedirect.com/science/article/pii/S0019057814003073>
- 20 C. Hwang and Y.-C. Cheng, "A numerical algorithm for stability testing of fractional delay systems," *Automatica*, vol. 42, no. 5, pp. 825 – 831, 2006.
- 21 J. Trigeassou, A. Benchellal, N. Maamri, and T. Poinot, "A frequency approach to the stability of fractional differential equations," *Transactions on Systems, Signals & Devices (TSSD)*, vol. 4, no. 1, pp. 1 – 25, 2009.
- 22 J. Sabatier, C. Farges, and J.-C. Trigeassou, "A stability test for non-commensurate fractional order systems," *Systems & Control Letters*, vol. 62, no. 9, pp. 739 – 746, 2013.
- 23 Z. Jiao and Y. Q. Chen, "Stability of fractional-order linear time-invariant systems with multiple noncommensurate orders," *Computers & Mathematics with Applications*, vol. 64, no. 10, pp. 3053 – 3058, 2012, advances in FDE, III. [Online]. Available: <http://www.sciencedirect.com/science/article/pii/S0898122111008789>
- 24 J. Trigeassou, N. Maamri, J. Sabatier, and A. Oustaloup, "A Lyapunov approach to the stability of fractional differential equations," *Signal Processing*, vol. 91, no. 3, pp. 437 – 445, 2011, advances in Fractional Signals and Systems. [Online]. Available: <http://www.sciencedirect.com/science/article/pii/S0165168410001854>
- 25 W. Chen, H. Dai, Y. Song, and Z. Zhang, "Convex lyapunov functions for stability analysis of fractional order systems," *IET Control Theory Applications*, vol. 11, no. 7, pp. 1070–1074, 2017.
- 26 H.-S. Ahn and Y. Chen, "Necessary and sufficient stability condition of fractional-order interval linear systems," *Automatica*, vol. 44, no. 11, pp. 2985 – 2988, 2008. [Online]. Available: <http://www.sciencedirect.com/science/article/pii/S0005109808002562>
- 27 M. Gora and D. Mielczarek, "Comments on "necessary and sufficient stability condition of fractional-order interval linear systems" [automatica 44 (2008), 2985–2988]," *Automatica*, vol. 50, no. 10, pp. 2734 – 2735, 2014. [Online]. Available: <http://www.sciencedirect.com/science/article/pii/S000510981400329X>
- 28 J.-G. Lu and Y. Chen, "Robust stability and stabilization of fractional-order interval systems with the fractional order  $\alpha$ : The  $0 \ll \alpha \ll 1$  case," *Automatic Control, IEEE Transactions on*, vol. 55, no. 1, pp. 152–158, Jan 2010.
- 29 Y. Yu and Z. Wang, "A graphical test for the interval stability of fractional-delay systems," *Computers & Mathematics with Applications*, vol. 62, no. 3, pp. 1501 – 1509, 2011, special Issue on Advances in Fractional Differential Equations [II]. [Online]. Available: <http://www.sciencedirect.com/science/article/pii/S0898122111002306>
- 30 B. Aguiar, T. Gonzalez, and M. Bernal, "Comments on "robust stability and stabilization of fractional-order interval systems with the fractional order  $\alpha$ : The  $0 < \alpha < 1$  case,"," *Automatic Control, IEEE Transactions on*, vol. 60, no. 2, pp. 582–583, Feb 2015.
- 31 Z. Gao and X. Liao, "Robust stability criterion of fractional-order functions for interval fractional-order systems," *Control Theory Applications, IET*, vol. 7, no. 1, pp. 60–67, Jan 2013.
- 32 Z. Gao, "Robust stability criterion for fractional-order systems with interval uncertain coefficients and a time-delay," *ISA Transactions*, vol. 58, pp. 76 – 84, 2015. [Online]. Available: <http://www.sciencedirect.com/science/article/pii/S0019057815001366>
- 33 —, "Robust stabilization criterion of fractional-order controllers for interval fractional-order plants," *Automatica*, vol. 61, pp. 9 – 17, 2015. [Online]. Available: <http://www.sciencedirect.com/science/article/pii/S0005109815003064>
- 34 L. Chen, R. Wu, Y. He, and L. Yin, "Robust stability and stabilization of fractional-order linear systems with polytopic uncertainties," *Applied Mathematics and Computation*, vol. 257, pp. 274 – 284, 2015. [Online]. Available: <http://www.sciencedirect.com/science/article/pii/S0096300314017640>
- 35 R. Mohsenipour and M. Fathi Jegarkandi, "Robust D-d-stability analysis of fractional order interval systems of commensurate and incommensurate orders," *IET Control Theory Applications*, vol. 13, no. 8, pp. 1039–1050, 2019.
- 36 I. Petras, Y. Q. Chen, B. Vinagre, and I. Podlubny, "Stability of linear time invariant systems with interval fractional orders and interval coefficients," in *Computational Cybernetics, 2004. ICC 2004. Second IEEE International Conference on*, 2004, pp. 341–346.
- 37 B. Senol, A. Ates, B. B. Alagoz, and C. Yeroğlu, "A numerical investigation for robust stability of fractional-order uncertain systems," *ISA Transactions*, vol. 53, no. 2, pp. 189 – 198, 2014. [Online]. Available: <http://www.sciencedirect.com/science/article/pii/S001905781300147X>
- 38 S. Zheng, "Robust stability of fractional order system with general interval uncertainties," *Systems & Control Letters*, vol. 99, pp. 1 – 8, 2017. [Online]. Available: <http://www.sciencedirect.com/science/article/pii/S0167691116301669>
- 39 H. Taghavian and M. S. Tavazoei, "Robust stability analysis of uncertain multiorder fractional systems: Young and jensen inequalities approach," *International Journal of Robust and Nonlinear Control*, vol. 28, no. 4, pp. 1127–1144, 2018. [Online]. Available: <https://onlinelibrary.wiley.com/doi/abs/10.1002/rnc.3919>
- 40 R. Malti, S. Victor, and A. Oustaloup, "Advances in system identification using fractional models," *Journal of Computational and Nonlinear Dynamics*, vol. 3, no. 2, pp. 021 401,1–7, 2008.
- 41 S. Victor, R. Malti, H. Garnier, and A. Oustaloup, "Parameter and differentiation order estimation in fractional models," *Automatica*, vol. 49, no. 4, pp. 926–935, 2013.
- 42 M. R. Rapačić and A. Pisano, "Variable-order fractional operators for adaptive order and parameter estimation," *IEEE Transactions on Automatic Control*, vol. 59, no. 3, pp. 798–803, March 2014.
- 43 R. Rapačić and R. Malti, "Stability of fractional incommensurate systems," in *International Conference on Fractional Differentiation and its Applications (ICFDA)*, Novi Sad, Serbia, 7 2016.
- 44 R. Malti and M. R. Rapačić, "Sufficient stability conditions of fractional systems with perturbed differentiation orders," in *20th IFAC World Congress*, Toulouse,

- France, 07 2017, pp. 14 557–14 562.
- 45 C. Bonnet and J. Partington, “Analysis of fractional delay systems of retarded and neutral type,” *Automatica*, vol. 38, no. 7, pp. 1133 – 1138, 2002.
  - 46 M. A. Pakzad, S. Pakzad, and M. A. Nekoui, “Exact method for the stability analysis of time delayed linear-time invariant fractional-order systems,” *IET Control Theory Applications*, vol. 9, no. 16, pp. 2357–2368, 2015.
  - 47 A. Mesbahi and M. Haeri, “Stability of neutral type fractional delay systems and its relation with stability of time-delay and discrete systems,” *IET Control Theory Applications*, vol. 10, no. 18, pp. 2482–2489, 2016.
  - 48 N. T. Thanh, H. Trinh, and V. N. Phat, “Stability analysis of fractional differential time-delay equations,” *IET Control Theory Applications*, vol. 11, no. 7, pp. 1006–1015, 2017.
  - 49 X. Zhang and Q. Zou, “Stability and stabilization of nonlinear fractional-order systems by lyapunov direct approach,” in *2017 36th Chinese Control Conference (CCC)*, July 2017, pp. 457–461.
  - 50 B. He, H. Zhou, Y. Chen, and C. Kou, “Asymptotical stability of fractional order systems with time delay via an integral inequality,” *IET Control Theory Applications*, vol. 12, no. 12, pp. 1748–1754, 2018.
  - 51 R. Malti, M. Aoun, F. Levron, and A. Oustaloup, “Analytical computation of the  $\mathcal{H}_2$ -norm of fractional commensurate transfer functions,” *Automatica*, vol. 47, no. 11, pp. 2425–2432, 2011.
  - 52 R. Malti, “A note on  $L_p$ -norms of fractional systems,” *Automatica*, vol. 49, no. 9, pp. 2923–2927, 2013. [Online]. Available: <http://www.sciencedirect.com/science/article/pii/S0005109813003166>
  - 53 E. Freitag and R. Busam, *Complex Analysis*, 2nd ed. London: Springer, 2009.
  - 54 M. Spivak, *Calculus*. London: Adison-Wesley, 1967.
  - 55 R. Malti, J. Sabatier, and H. Akçay, “Thermal modeling and identification of an aluminium rod using fractional calculus,” in *15th IFAC Symposium on System Identification (SYSID)*, Saint-Malo France, 7 2009, pp. 958–963.

## 8 Appendix

**Theorem A** (Rouché, [53]). *Let  $f$  and  $g$  be complex mappings, holomorphic inside and on a closed contour  $C$ . If  $g$  is strictly absolutely dominated by  $f$  on  $C$ , i.e. if*

$$|g(s)| < |f(s)| \quad (\forall s \in C) ,$$

*then  $f$  and  $f + g$  have the same number of zeros inside  $C$ , where each zero is counted according to its multiplicity.*